ELSEVIER

Surface and Coatings Technology 114 (1999) 224–229

SURFACE & COATINGS TECHNOLOGY

Ion energy and momentum flux dependence of diamond-like carbon film synthesis in radio frequency discharges

A.D. Glew [a,*], R. Saha [a], J.S. Kim [b], M.A. Cappelli [b]

[a] *Materials Science and Engineering Department, Stanford University, Stanford, CA, 94305 USA*
[b] *Thermosciences Division, Mechanical Engineering Department, Stanford University, Stanford, CA, 94305 USA*

Received 28 April 1998; received in revised form 4 February 1999; accepted 9 February 1999

Abstract

An investigation of the ion energy and ion momentum flux dependence of the properties of plasma-deposited diamond-like carbon (DLC) films is presented. The DLC films are deposited in low pressure radio frequency (RF) discharges operating at 13.3 Pa with methane as the source gas. The discharge is characterized in situ for the negative direct current (d.c.) self-bias voltage at the powered electrode, the average discharge current, and the total power, from which the average ion energy and average incident momentum flux can be determined. Ion energies explored in this study range from 50 to 250 eV. Films are deposited on [100] n-type silicon wafers and are characterized by a variety of analytical methods to determine film hardness, density, and stress. It is shown that the maximum film density (1.7 g/cm^3) and hardness (18 GPa) correspond to conditions of maximum deposition rate (5×10^{-6} g/s) and maximum film stress (1.8 GPa) all at ion energies of approximately 160 eV. These values are comparable with those previously reported in the literature. The relationship between film properties and impinging ion energy and ion momentum flux is discussed within the framework of existing models of diamond-like carbon formation. © 1999 Published by Elsevier Science S.A. All rights reserved.

Keywords: Diamond-like carbon; Film; Ion energy; Momentum flux; Radio frequency discharge; Synthesis

1. Introduction

Although Schmellenmeier first identified diamond-like phases of carbon in 1953 [1], their synthesis and properties have only recently been the subject of intense research. DLC films are metastable phases of carbon, containing typically 20–60% sp^3 bonds. It is this relatively large sp^3 bond component that imparts the many diamond-like properties. The films are mechanically hard [2,3], transparent in the infrared (IR) [4–6], have a low sliding friction coefficient [7] and a variable band-gap. DLC film hardness can approach 20 or 30 GPa, making them attractive in applications such as wear-resistant coatings for magnetic [8], optical, and biomedical devices [9]. Others have proposed the use of DLC flat panel displays [10].

Certain DLC film properties have impeded their use in many of these applications [9]. The relatively low temperature limitation, 300°C [11], makes them impractical in many applications, most notably, as a dielectric in integrated circuits when there are subsequent high temperature processes or as metal cutting tools. DLC films also exhibit compressive stresses, in the range of 1–10 GPa [12], which are greater than the stresses in dielectric films, 0.3–0.7 GPa [13]. Reducing the intrinsic stress without compromising the other properties of the films is desirable in most applications. However, a minimum film stress appears to be necessary in order to impart the hard diamond-like properties that make DLC a useful coating [14,15]. Films deposited with lower values of stress are usually polymeric or highly graphitic.

DLC films can be deposited by a wide variety of methods. These include plasma-enhanced chemical vapor deposition (PECVD), magnetron and radio frequency (RF) sputtering, arc evaporation, and laser ablation [16,17]. A common feature in all of these deposition methods is that hydrocarbon ions strike a substrate with impact energies ranging from a few to several hundred electron volts. Theories that explain the metastable synthesis of DLC films include preferential etching of sp^2-bonded carbon due to ion bombardment

* Corresponding author. Tel.: +1-650-723-1823; fax: +1-650-723-1748.
E-mail address: adglew@leland.stanford.edu (A.D. Glew)

0257-8972/99/$ – see front matter © 1999 Published by Elsevier Science S.A. All rights reserved.
PII: S0257-8972(99)00061-4

[18] and film densification due to knock-on or low energy ion subplantation [19]. It is believed that at sufficiently high energies, the energetic ions can produce a thermal spike upon impact, which can cause the relaxation and transformation of sp^3 bonds to sp^2 bonds.

The structure and composition of these films can vary depending on processing parameters. For example, in RF discharge PECVD, the film properties are seen to depend on discharge parameters such as the negative bias voltage established at the powered electrode, operating pressure, temperature, and gas precursor [20]. Although it is desirable to develop a molecular-level understanding of the DLC deposition process, in many deposition methods, the molecular deposition properties are related to the macroscopic process conditions in a complex way. In RF discharge PECVD, the RF power and operating pressure determine the self-bias and impinging ion energy distribution. While parametric studies of deposition conditions afford the development of process recipes, it is the development of an understanding of the molecular properties of the deposition method that offer insight as to the mechanism for film formation.

In this paper, we report on our initial investigations on the role that energetic ion bombardment plays in the formation and stabilization of sp^3 bonds in RF discharge PECVD of carbon films. For a limited range of processing conditions, we have characterized the plasma for impinging average ion energy and ion momentum flux, and have systematically studied the effects that these parameters have on film properties such as stress, density, and hardness.

2. Experiment

The low pressure capacitively-coupled RF discharge apparatus employed in this study is schematically illustrated in Fig. 1. The RF discharge is sustained in a grounded 12 inch diameter vacuum chamber constructed of stainless steel. The substrates are placed on the lower, 150 mm diameter powered electrode located a distance of approximately 100 mm from the upper, grounded electrode. Power is delivered to the lower electrode from a 13.56 MHz RF generator and tunable impedance matching network. The power delivered to the plasma is monitored with a power meter (Bird Model 43), the discharge current, I_{rms}, with a Hall probe (Pearson Model 2878), and the discharge voltage with a high voltage probe. Following Lee et al. [21] and Catherine and Couderc [22], the mean plasma potential, V_p, is estimated from the peak to peak voltage, V_{pp}, and the d.c. self-bias voltage, V_{dc}, as:

$$V_p = \frac{1}{2}(V_{pp} + V_{dc}). \tag{1}$$

The values of V_{pp} and V_{dc} are read directly from the voltage probe trace displayed on a digital oscilloscope. The maximum ion energy is expected to be $\epsilon_{imax} = e(V_p - V_{dc})$, with e the electron charge. Since $|V_{dc}| \gg V_p$, the maximum ion energy $\epsilon_{imax} \approx eV_{dc}$. The actual ion energy, ϵ_i, may be significantly lower than this in a collisional plasma sheath, depending on the ratio of the mean free path to the sheath thickness. At a discharge pressure of 13.3 Pa, the plasma is weakly collisional and the ions are expected to suffer momentum-changing collisions. The average ion energy is approximated as [21]:

$$\epsilon_i = e\frac{V_p - V_{dc}}{d_{sp}}\lambda\cos(\alpha). \tag{2}$$

Here, λ is the ion collision mean free path, d_{sp} is the sheath thickness, and $\cos(\alpha)$ is a factor of value close to 0.5 when the ion and neutral collision partner are close in size [23]. The sheath thickness at the powered electrode is given as [21]:

$$d_{sp} = \frac{(V_p - V_{dc})\omega\epsilon_0 A_p}{I_{rms}}. \tag{3}$$

Here, ω is the discharge frequency, A_p is the powered electrode area, and ϵ_0 is the vacuum permittivity. A typical sheath thickness as calculated from Eq. (3) using measured discharge parameters for a discharge power and pressure of 30 W and 13.3 Pa, respectively, is $d_{sp} \approx 1$ mm. A conservative estimate of the momentum-transfer mean free path, obtained using a hard sphere approximation for methane ions colliding with neutral methane, gives $\lambda \approx 1$ mm. However, charge-transfer cross-sections are likely to be greater than hard sphere cross-sections, and would make the sheath more collisional than estimated here. Our estimates of the ion energies use a simple hard sphere model and so should be interpreted as upper bounds in this study. The ion flux, Γ_i, is determined from the flux of ion current, J_i [21]:

$$\Gamma_i = \frac{J_i}{e} = \frac{I_{rms}\sqrt{2}}{e\pi A_p\left[1 - \frac{1}{\pi}\cos^{-1}\left(\frac{-V_{dc}}{\frac{1}{2}V_{pp}}\right)\right]}. \tag{4}$$

The ion momentum flux is then calculated as $\Gamma = \Gamma_i\sqrt{2m_i\epsilon_i}$, where m_i is the mass of the dominant ionic species (assumed to be CH_4^+) transported across the sheath. In general, the ion mean free path depends on the collision cross-section, which can vary with ion energy. For the results presented here, we assume that the methane ion collision cross-section (and hence mean free path) is a constant.

The powered electrode (on which the substrate sits) is water-cooled. The substrates are cleaned by argon ion bombardment at an RF power density of 0.57 W/cm^2,

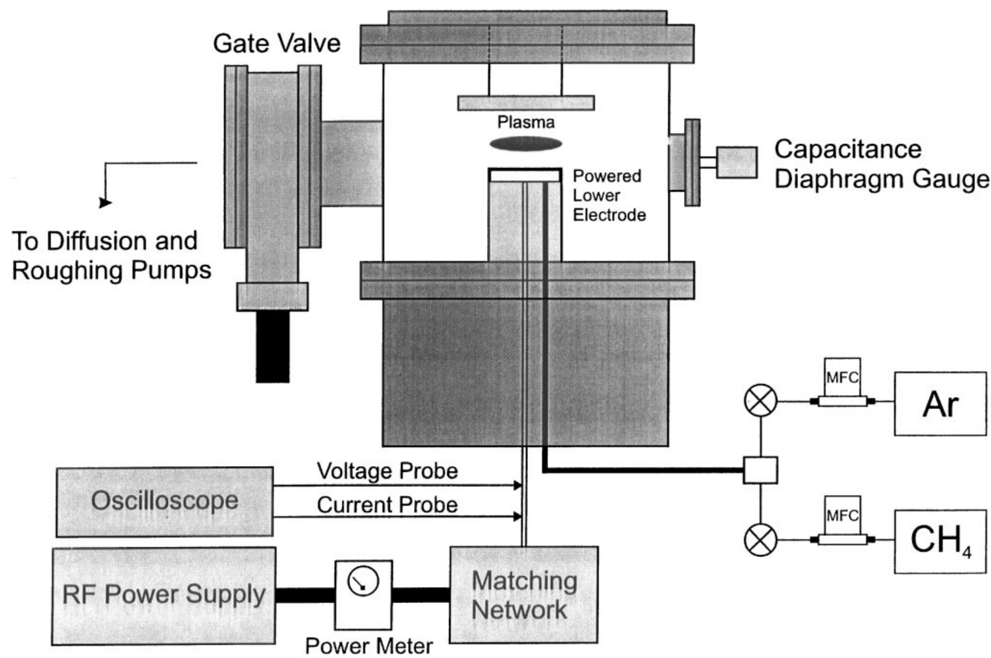

Fig. 1. Schematic of low pressure capacitively-coupled RF discharge apparatus.

a d.c. self-bias voltage of approximately 375 V, and a pressure of 13.3 Pa for 5 min prior to deposition to remove adsorbed surface contamination.

The carbon chemistry in the films is analyzed by electron spectroscopy for chemical analysis (ESCA). Profilometers are used to examine the surface morphology and film thickness. The film weight is determined by measuring the sample before and after deposition with a Mettler AE240 scale. Film stress is determined by measuring the pre- and post-deposition curvature of the silicon wafers using laser reflectometry [24]. The stress is calculated from the change in curvature of the substrate using the Stoney thin film approximation:

$$\sigma_{\mathrm{f}} = \frac{M_{\mathrm{s}} t_{\mathrm{s}}^{2}}{(6 t_{\mathrm{f}} R)}. \tag{5}$$

Here, M_s is the substrate biaxial modulus, R is the post-deposition increase in wafer curvature, and t_s and t_f are the substrate and film thicknesses, respectively.

Nano-indentation studies are performed with a Nano Indenter II (MTS Systems Corp.) microprobe instrumented with a Berkovich indenter. The displacements into the films were made using a constant displacement loading rate in the load segment to a specified depth of 90, 100, and 120 nm. Each measurement was repeated three times. Film hardness was extracted from the load–displacement curves using the method of Oliver and Pharr [25]. A fused silica sample functions as a reference standard to ensure that the measured hardness values were reasonable.

3. Results and discussion

The carbon (1s) binding energies for diamond and graphite are 287 and 284 eV, respectively. In the past, researchers [26] have used ESCA to identify diamond content in DLC films deposited in methane plasmas. ESCA spectra (variation in the X-ray photoelectron counts as a function of the binding energy) of the films deposited at incident ion energies of 96, 98, 120, 165, and 211 eV in this current experiment are shown in Fig. 2. The characteristic C (1s) binding energies of the two samples deposited at 96 eV (135 nm thick film) and 120 eV (240 nm thick film) appear 1 eV greater than the

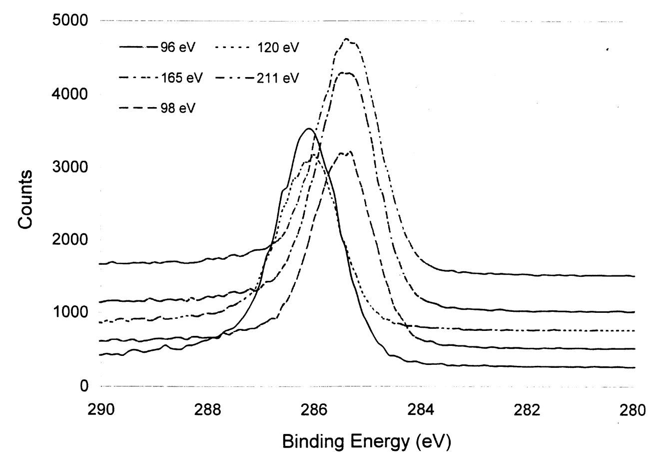

Fig. 2. ESCA spectra of DLC films at 13.3 Pa for a range of average ion energies.

other samples. A shift of the C (1s) peak towards higher energy can arise if these films have a higher binding energy than the other samples. A shift can also be the result of sample charging. If a net positive charge accumulates on the sample surface, then it will attract the emitted photoelectrons, making the material appear to have a higher binding energy. Thus, materials with a lower dielectric constant will charge and show an apparent shift of the binding energy to higher values. The effect of sample charging can be studied by exposing the sample during analysis with electrons to neutralize the charging effect. The two samples which showed an apparently higher binding energy did in fact exhibit charging. The apparent binding energy decreased when the insulating samples were re-examined with the charge neutralization electron gun in operation. It is noteworthy that these two films had stresses and densities that were among the highest measured. It is also noteworthy that the sample deposited at 98 eV of ion energy (388 nm thickness) but for a deposition time that was twice that of the 135 nm thick sample (similar deposition conditions) did not show a shift due to charging. Experiments consistently showed that the deposition rate increases with film thickness, as is apparent in this particular case. For example, in one study, films were deposited at fixed power and pressure (30 W and 13.3 Pa) for deposition times of 480, 600, 900, and 1200 s. Over this range, the deposition rates were seen to increase monotonically from 3.4 to 5.1 μg/s.

Only the thinner of the two samples (135 nm and 388 nm) deposited under the same conditions (approximately 97 eV average ion energy) showed significant charging. The deposition time doubled, but there was also an apparent 40% overall increase in the mass deposition rate. Similarly, a 600 s deposition resulted in a 50% greater mass deposition rate than a 240 s deposition. The increase in deposition rate with time saturated after 600 s. The change in deposition rate and charging with thickness certainly warrants further study. This result, however, may not be unusual in the synthesis of diamond-like carbon films. Using Fourier transform infrared spectroscopy, Crouse [27] showed that DLC properties had an apparent increase in the sp^3 to sp^2 bond ratio with thickness above 50 nm. Furthermore, Hirakuri et al. [28] showed a dependence of film stress on thickness in the 200–1500 nm range.

The variation in the calculated average ion energy and ion momentum flux with discharge power is shown in Fig. 3, for a 13.3 Pa (100 mTorr) discharge pressure in pure CH_4. The ion energy and ion momentum flux are seen to increase monotonically with the transmitted power at a fixed pressure. While a more complex relationship for the variation in the average ion energy (and negative bias voltage) with pressure at a constant power is expected and has been recorded, only conditions of constant pressure are reported in this study. Although

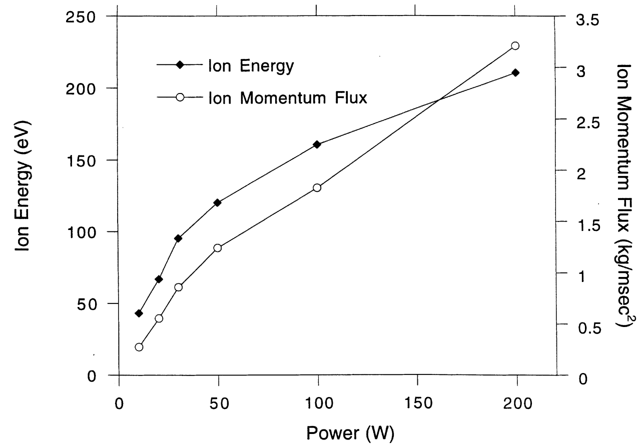

Fig. 3. Variation in the calculated average ion energy and ion momentum flux with discharge power.

the average ion energy is expected to be a determinant in the stabilization of sp^3 bonds in carbon films, it is speculated that the process depends also on the total rate of energy or momentum transfer to the film during deposition. In a similar process of energetic ion-enhanced deposition of cubic boron nitride films, it has been seen that the complex deposition process scales best with the ion momentum flux on a per atom deposited basis [29]. Also, Hoffman and Gaettner [30] found the stress in films to correlate with transfer of ion momentum during chromium deposition. It is noteworthy here to mention that while the precise mechanism for deposition is not yet known, our measured ion currents suggest that the ion flux to the surface is sufficient to account for the observed film deposition rates, and therefore a subplantation model is plausible [19].

The variation in film stress and hardness with average incident ion energy is shown in Fig. 4. The variation of these properties with incident ion momentum flux would be qualitatively similar, and can be inferred from the

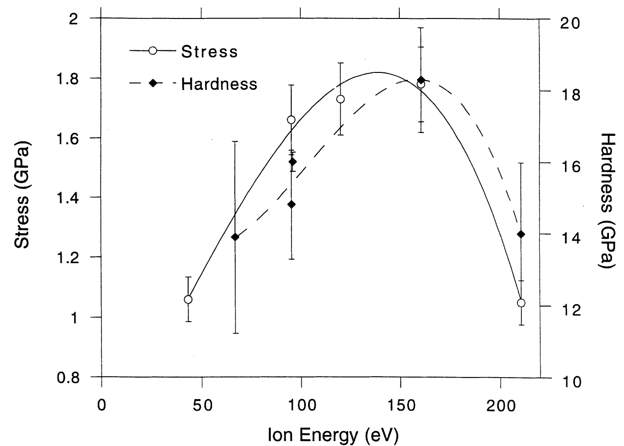

Fig. 4. Variation in film stress and hardness with calculated average ion energy.

relationship between the ion momentum flux and energy shown in Fig. 3. The film stress, which is seen to be compressive, initially increases with increasing ion energy, peaks at a maximum of approximately 150 eV (to a value of approximately 1.8 GPa), and then drops significantly at higher energies. The dependence of film stress on ion energy (and hence self-bias voltage) follows a pattern seen in prior studies [14]. The value of the peak stress, 1.8 GPa, observed here is similar to that seen in studies by Crouse [27] and Hirakuri et al. [28].

The film hardness values determined from our nano-indentation studies shown in Fig. 4 are the average of the three readings taken for maximum consecutive load displacements of 90, 100 and 120 nm. The error bars represent one standard deviation in the data. In all but one sample, the scatter in the resulting hardness values is significant (>10%). The hardest film deposited (18 GPa) corresponded to the highest intrinsic stress as seen by others [31].

The variation in the measured film density and deposition rate with incident average ion energy is shown in Fig. 5. Plotting the variation of these properties with varying ion momentum flux would give a qualitatively similar trend, as can be inferred from Fig. 3. All three properties are seen to peak at the conditions of ion energy where the highest stress is observed. The film densities are within the range of 1.6–2.2 g/cm^3 typical for hard hydrogenated amorphous carbon (a:C–H) [32]. The dependence of film density on ion energy (and hence self-bias voltage) follows a pattern seen in prior studies [17]. However, the films are much less dense than the 2.9 g/cm^3 reported by Cuomo et al. [33] for diamond-like carbon films deposited from hydrogen-free sources with a high sp^3 content (80%).

The film deposition rates range from 1.2×10^{-6} to 9.3×10^{-6} g/s, typical of rates for DLC films deposited by the PECVD method [34]. For the results reported here, the deposition rates peak at an average ion energy of approximately 160 eV, and then decline as the incoming ions begin to sputter the film.

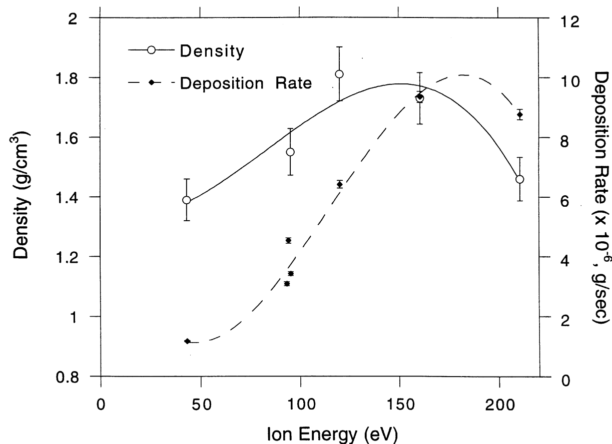

Fig. 5. Variation in film density and deposition rate with calculated average ion energy.

These data provide further confirmation that the mechanism responsible for DLC deposition in RF plasma discharges is through a knock-on or ion subsurface penetration. In this process [35], the incident low energy ions displace surface atoms (through a forward sputtering mechanism) into interstitial sites, or penetrate the surface themselves. This is consistent with the observed increase in stress, density, and hardness with average ion energy. The subsurface penetration probability has been shown to reach near unity values at about the average ion energy where our film densities reach a maximum value (about 160 eV). It is expected that this process will have a penetration threshold energy [19]. Furthermore, the decrease in density above this energy is consistent with a thermal relaxation of the film as energetic ions cause atoms to relax at a rate that is proportional to $\epsilon_i^{5/3}$ [19,35].

4. Conclusions

In this study, DLC films were deposited in low pressure RF discharges with CH_4 as the source gas. The bias voltage at the powered electrode, average ion current, and total power were monitored, and the average ion energy and ion momentum flux were estimated from these measurements. The as-grown films were analyzed by a wide variety of analytical methods to determine the film properties such as stress, density, and hardness. The results show that the maximum film density and hardness correspond to the maximum film stress all at average ion energies of approximately 160 eV. The C (1s) peak shifted to higher binding energies only for the thinnest films deposited at approximately 100 eV. The apparent peak shift was due to sample charging, resulting from decreased dielectric constant. This warrants direct examination of the dielectric properties of the material, which the authors will explore. The deposition rate increased with thickness, and then saturated. The compressive film stress ranged from 1.05 to 1.8 GPa for DLC films deposited with ion energies ranging from 96 to 211 eV. The hardness reached 18 GPa under the conditions of 160 eV.

Acknowledgements

The initial funding for this research was provided by LG Electronics. The authors would like to thank Millipore Corporation for their equipment contributions. The authors would like to thank Professor W.D. Nix for use of the nano-indenter.

References

[1] M. Schmellenmieier, Z. Phys. Chem. 205 (1955) 349.
[2] M. Tamor, in: A. FeldmanY. Tzeng, W.A. Yarbrough, M. Yoshikawa, M. Murakawa (Eds.), Proc. 3rd Int. Conf. on Applications of Diamond Films and Related Materials, NIST Special Publication 885, NIST, Gaithersburg, MD, 1995, p. 691.
[3] S. Bull, Diamond Relat. Mater. 4 (1995) 827.
[4] N. Savides, J. Appl. Phys. 59 (1986) 4133.
[5] G. Clarke, R. Parsons, Thin Solid Films 236 (1993) 67.
[6] F. El-Hossary, D. Fabian, C. Sofield, Thin Solid Films 157 (1988) 34.
[7] A. Gangopadhyay, P.A. Willermet, M.A. Tamor, W.C. Vassell, in: A. FeldmanY. Tzeng, W.A. Yarbrough, M. Yoshikawa, M. Murakawa (Eds.), Proc. 3rd Int. Conf. on Applications of Diamond Films and Related Materials, NIST Special Publication 885, NIST, Gaithersburg, MD, 1995, p. 703.
[8] H. Nakue, T. Mitani, H. Kurokawa, T. Yonezawa, H. Yoshio, Thin Solid Films 212 (1992) 240.
[9] J. Lettington, Philos. Trans. Roy. Soc. London A 342 (1993) 287.
[10] F.J. Clough, B. Kleinsorge, W.I. Milne, J. Robertson, Mater. Res. Soc. Symp. Proc. 423 (1996) 39.
[11] J. Parmeter, D. Tallant, M. Siegal, Mater. Res. Soc. Symp. Proc. 349 (1994) 513.
[12] K. Lee, Y. Baik, K. Eun, Mater. Res. Soc. Symp. Proc. 308 (1993) 101.
[13] S. Wolfe, R. Tauber, Silicon Processing for the VLSI Era, Lattice Press, Sunset Beach, CA, USA, 1986, p. 228.
[14] E. Dekempener, R. Jacobs, J. Smeets, J. Meneve, L. Eersels, B. Blanpain, J. Roos, D. Oostra, Thin Solid Films 217 (1992) 56.
[15] M. Chhowalla, J. Chen, B. Kleinsorge, J. Robertson, G. Amapatunga, W. Milne, Mater. Res. Soc. Symp. Proc. 423 (1996) 299.
[16] M. Paterson, K. Orrman-Rossiter, D. Sood, S. Bhargava, Diamond Relat. Mater. 2 (1993) 1439.
[17] M. Weiler, S. Sattel, K. Jung, H. Ehrhadt, V. Veerasamy, J. Robertson, Appl. Phys. Lett. 64 (1994) 2797.
[18] J. Robertson, Philos. Trans. Roy. Soc. London A 342 (1993) 277.
[19] J. Robertson, Diamond Relat. Mater. 3 (1994) 361.
[20] A. Grill, V. Patel, Diamond Relat. Mater. 4 (1994) 62.
[21] J.H. Lee, D.S. Kim, Y.H. Lee, B. Farouk, J. Electrochem. Soc. 143 (1996) 1451.
[22] Y. Catherine, P. Courderc, Thin Solid Films 144 (1986) 265.
[23] G.H. Wannier, J. Bell System Tech. 49 (1953) 170.
[24] P.A. Flinn, D.S. Gardner, W.D. Nix, IEEE Trans. Electron Dev. ED-34 (1987) 689.
[25] W.C. Oliver, G.M. Pharr, J. Mater. Res. 7 (1992) 1564.
[26] O. Matsumoto, H. Toshima, Y. Kanzaki, Thin Solid Films 128 (1985) 341.
[27] P. Crouse, Diamond Relat. Mater. 2 (1993) 885.
[28] K.K. Hirakuri, T. Minorikawa, G. Friedbacher, M. Grasserbauer, Thin Sold Films 302 (1997) 5.
[29] P.B. Mirkarimi, K.F. McCarty, D.L. Medlin, W.G. Wolfer, T.A. Friedman, E.J. Klaus, G.F. Cardinale, D.G. Howitt, J. Mater. Res. 9 (1994) 2925.
[30] D. Hoffman, M. Gaettner, J. Vac. Sci. Technol. 17 (1980) 415.
[31] M. Tamor, W. Vassell, K. Carduner, Appl. Phys. Lett. 58 (1991) 592.
[32] J. Robertson, Surf. Coat. Technol. 50 (1992) 185.
[33] J.J. Cuomo, J.P. Doyle, J. Bruley, J.C. Liu, Appl. Phys. Lett. 58 (1991) 466.
[34] P. Koidl, C. Wild, B. Dischler, J. Wagner, M. Ramsteiner, Mater. Sci. Forum. 52 (1990) 41.
[35] C. Davis, Thin Solid Films 226 (1993) 30.